TARGET THICKNESS AND UNIFORMITY MEASUREMENTS USING DOUBLE SIDED SILICON STRIP DETECTORS

Ioana KUNCSER [1,2], Catalin MATEI [1,2,*], Teodora PETRUSE [1]

The thickness of a material with a known stoichiometry can be evaluated by measuring the energy loss of the alpha particles emitted by a known source after passing through the dissipative medium. The energy loss can be measured and mapped by using double sided silicon strip detectors (DSSSD). The proposed procedure was applied to estimate the thickness of three targets, each consisting in a LiF layer deposited on Mylar substrate. The description of the experimental set-up along with the results of the measurement are presented in this paper. The targets have been recently used to study the ^{7}Li photodisintegration.

Keywords: silicon detectors, charged particles, energy loss.

1. Introduction

In nuclear physics experiments a reaction is usually studied through the interaction of a specific beam with a specific target, followed by the detection of the reaction products. The characteristics of the beam and of the target will strongly influence the reaction rate [1]. Therefore, a proper knowledge of the beam intensity and energy, and of the target composition, thickness, and uniformity is mandatory for an accurate final result. This work reports an accessible procedure to estimate the thickness and the uniformity of a target with a known stoichiometry based on measuring the energy loss of alpha particles emitted by a known source after passing through the target. The experimental set-up consists of components available in any nuclear physics laboratory: DSSSDs, standard alpha sources and basic data acquisition chains. Similar measurements have been reported before, in general being performed with ion-implanted Si detectors [2-3] or surface barrier Si detectors [4] and collimated alpha sources.
The procedure was applied to measure the thickness of three targets which have been used in a nuclear physics experiment. Each of those consists in a LiF layer deposited on a Mylar substrate. A reference substrate has been evaluated separately.

[1] Extreme Light Infrastructure – Nuclear Physics (ELI-NP), Horia Hulubei National Institute for R&D in Physics and Nuclear Engineering (IFIN-HH), 077125 Bucharest-Magurele, Romania
[2] Doctoral School in Engineering and Applications of Lasers and Accelerators, National University of Science R&D Technology POLITEHNICA Bucharest, 060042 Bucharest, Romania
* Corresponding author: e-mail: catalin.matei@eli-np.ro

The results of those measurements will be reported in this paper. The three targets were used to study the ^{7}Li photodisintegration cross section at the High Intensity γ-ray Source (HIγS) from Duke University [5]. The reaction products, alpha particles and tritons, were detected in coincidence using a silicon detector array SIDAR [6]. The thickness and the uniformity of the LiF layers is essential to evaluate the number of ^{7}Li atoms involved in the reaction and further the cross-section.

The LiF targets were provided by the Target Laboratory of LNS (INFN) [7] and their thicknesses were measured at the "Detector and Spectroscopy Laboratory" at ELI-NP [8].

2. Theoretical concepts

Charged particles are losing energy while crossing through matter, especially due to the interactions with the electrons, being finally stopped at a precise thickness – the Stopping Range (SR). The energy loss in the unit of thickness is characteristic to each material and is evaluated by the Stopping Power S(E). The Bethe-Bloch formula is expressing this quantity by multiplying the energy transferred in an interaction with the number of electrons encountered in the unit of length [9-10]:

$$S(E) = -\frac{dE}{dx} = \frac{4\pi z^2 e^4}{mV^2} \cdot N \cdot Z \cdot ln\frac{2mv^2}{I} \quad (1)$$

where z is the electric charge of the incident particle (in units of e), v is the velocity of the incident particle, m is the mass of the electron, and I is the average excitation/ionization potential.

According to eq. (1), if the type and the energy of the incident particles are known, the precise thickness of a certain material can be determined by measuring the energy of the transmitted particles. The energy loss in a material with a thickness t < SR, is the following [11]:

$$E_{loss} = \int_0^t \frac{dE}{dx} dx \quad (2)$$

Furthermore, if t << SR → S(E) ~ const. Thus,

$$E_{loss} = \frac{dE}{dx} \cdot t \quad (3)$$

Currently, there are several software packages based on Monte Carlo simulations which can estimate the S(E) of both simple and complex materials and to perform energy loss calculations: GEANT4 [12], SRIM/TRIM [13], LISE++ [14], PENELOPE (for positrons and electrons) [15], etc.

3. Experimental set-up and method

The experimental set-up was assembled inside a spherical vacuum chamber using an ^{241}Am - ^{239}Pu - ^{244}Cm alpha source, emitting particles at 5.155 MeV, 5.486 MeV and 5.805 MeV, and a DSSSD (Mirion Model PF-16CT-16CD) detector. The

DSSSD has 16 strips on the junction side and 16 strips on the ohmic side, as presented in Fig. 1 [16]. A pressure between 5×10^{-6} mbar and 1×10^{-5} mbar was maintained during the experiment inside the spherical vacuum chamber using a turbomolecular pump station. The incoming signal is processed by an electronic chain consisting of two Mesytec MPR-16 preamplifiers, two Mesytec MSCF-16 shaping/timing filter amplifiers, an Ortec GG8020 gate generator, a Mesytec 32 channel Peak Sensing ADC MADC32 and a VME controller SIS3153. The data are acquired using "mvme" Mesytec VME DAQ [17-18]. The design of the electronic chain is presented in Fig. 2.

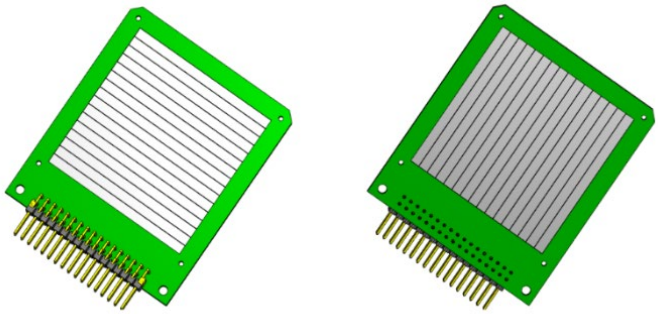

Fig. 1. CAD design of Mirion Model PF-16CT-16CD DSSSD

The experimental set-up has been implemented to measure the thickness of three LiF layers deposited by thermal evaporation on three similar Mylar substrates. In advance, an empty Mylar substrate was measured as a reference thickness. The empty substrate and the LiF targets were mounted on a holder which was attached upside down to the top of the vacuum chamber. The substrate occupies the lowest spot, being followed by the targets on the next three superior spots. A small deviation of the target holder from the vertical plane was noticed during the measurements and considered in the final result. The alpha source was placed as close as possible to the plan of the target holder (~1cm) and oriented towards the center of the DSSSD. The substrate and the targets were successively placed between the source and the detector, using a linear manipulator. The energy of the outgoing alpha particles was measured for each spot occupied on the target holder.

The distance between the plane of the source and the plane of the detector was around 6 cm. The configuration inside the vacuum chamber and the expected profile of the detected energy are illustrated in Fig. 4.

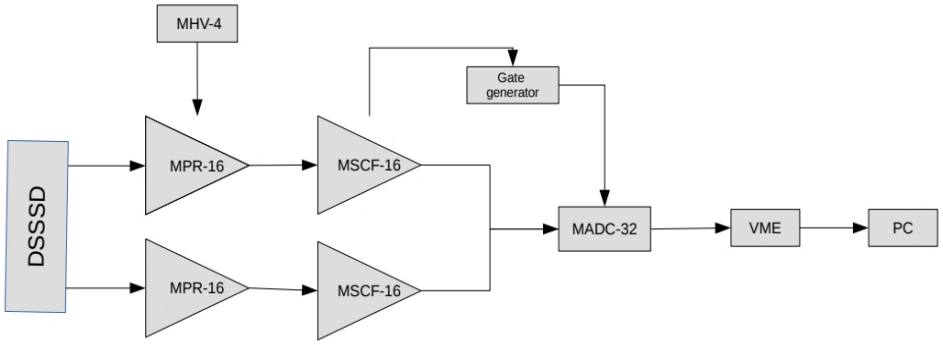

Fig. 2. The design of the electronic chain used for thickness measurement

Following the measurement were obtained 16 spectra from the front side and 16 spectra from the rear side of the DSSSD without any target, with the substrate and with each target. The spectral behavior for each of those situations is represented in Fig. 3. All spectra correspond to the eighth strip from the front side of the DSSSD, thus to the center of the detector. It can be noticed how the alpha particles are losing energy in the substrate, respectively in the target. However, the representation is just qualitative because the substrate and the target weren't placed exactly in the same position. Another observation is related to the energy resolution. As the resolution was expected to increase as more material is placed between the source and the detector, the acquisition time was increased once for the substrate and once more for the targets (as it can be noticed from the number of counts). However, even with this increasement of the acquisition time, the deterioration of the energy resolution is noticeable.

All the data were processed using a C++ code together with the Octave software [19] for the graphical representation. For each strip, the code separates the three peaks and computes the mean of the Gaussian distribution described by each peak. The uncertainty of the mean will be taken in account as a statistical uncertainty. Further, the empty frame spectra are calibrated using the three known energies of the alpha source and then the spectra with substrate or with target are calibrated using the same parameters. After the calibration, the statistical uncertainty is around 0.4 keV. The uncertainty induced by the fit used for the energy calibration is neglectable (less than 0.1 keV).

For each peak, the mean value between the energy detected in the junction side and in the ohmic side was calculated and represented for all the 256 pixels of the DSSSD. The discrepancies between those two values are leading to a systematic uncertainty (few keV). Therefore, for each pixel will correspond an energy loss value determined with a precision imposed by the sum between the statistic and the

systematic uncertainty. In the case of the three targets, the so evaluated uncertainty will be summed with the uncertainty of the energy loss in the substrate.

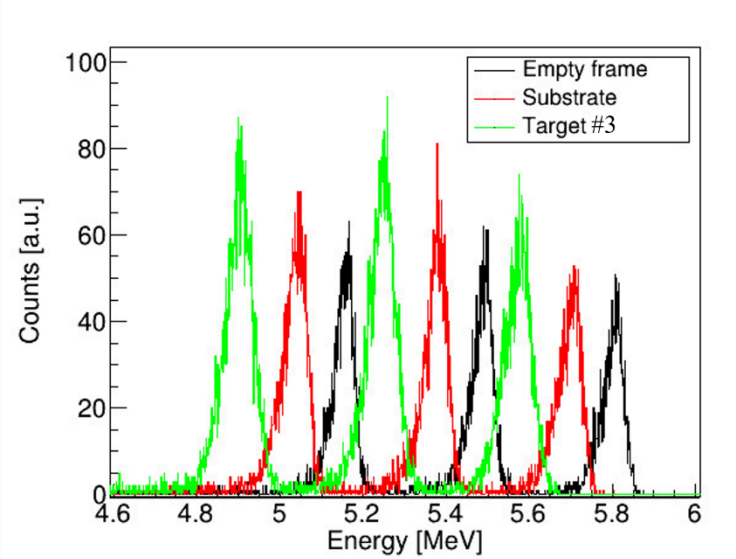

Fig. 3. A typical spectrum measured without any target (black), with the substrate (red) and with target (green). All spectra are corresponding to the same strip from the front side.

The conversion of the energy units in length units was performed using LISE++ and STRIM stopping power values. The conversion of the energy uncertainties in thickness uncertainties was performed by estimating the thickness at the limits of energy loss interval.

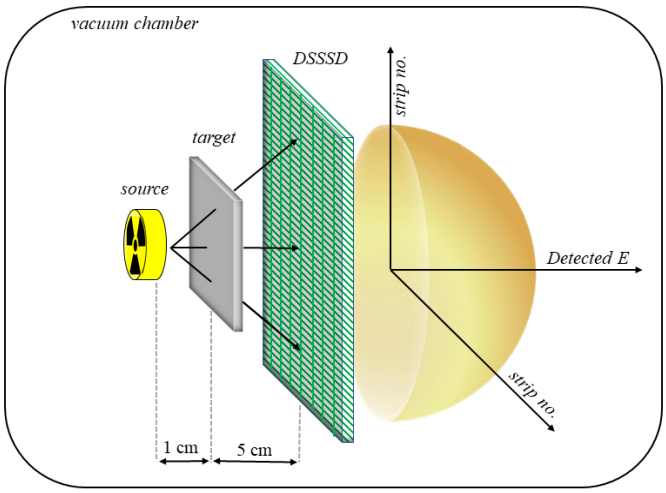

Fig. 4. The configuration inside the vacuum chamber (image not to scale)

4. Results

The alpha particles, which are emitted isotropically by the source, are incident on the target at different angles and are traversing different paths, suffering different energy losses. Therefore, as presented in Fig. 4, for a uniform target the mapping of the detected energy shows a cupola-like shape. The maximum (top of the cupola) corresponds to the normal incidence of the alpha particles on the target. Equivalently, by mapping the energy loss, the resulted surface will present a minimum. Those local extrema are corresponding to the shortest path of the alpha particles through the target, allowing an accurate estimation of the thickness. Moreover, the smoothness of those calculated surfaces confers a qualitative evaluation of the uniformity of the material under study. A quantitative evaluation can be reached by angular corrections if the geometry is well defined. The thickness of the LiF layers was evaluated by subtracting the energy loss in the reference Mylar substrate.

The deviation of the target holder from the vertical plane has a strong impact over the results of the measurement. However, as long as the detected energy, respectively the energy loss, are mapped for the entire detector and the maps are presenting a maximum, respectively a minimum, the target thickness can be accurately estimated despite the possible misalignments. Therefore, the deviation between the surface of the targets and the surface of the detector didn't affect the final result. This aspect is highlighting the advantage of using DSSSD detectors for thickness measurements instead of conventional ion-implanted Si detectors.

4.1 The measurement of the thickness of the Mylar substrate

The detected energy and the energy loss in the substrate were mapped for each energy of the alpha source. The results are presented in Fig. 5. The substrate occupied the lowest spot on the target holder and suffered the strongest deviation. Hence, the shortest path of the alpha particles through the substrate corresponds to the energy detected in the peripherical strips of the DSSSD. It's important to specify that a larger deviation would have led to an invalid result due to the impossibility to identify the local extrema. A similar behavior is expected when the target and the detector are perfectly aligned, but the target presents a strong thickness gradient. Unfortunately, due to the visible deviation of the target holder, the presence of such a gradient cannot be confirmed. However, the method can still reveal the presence of local non-uniformities, as small valleys and bumps.

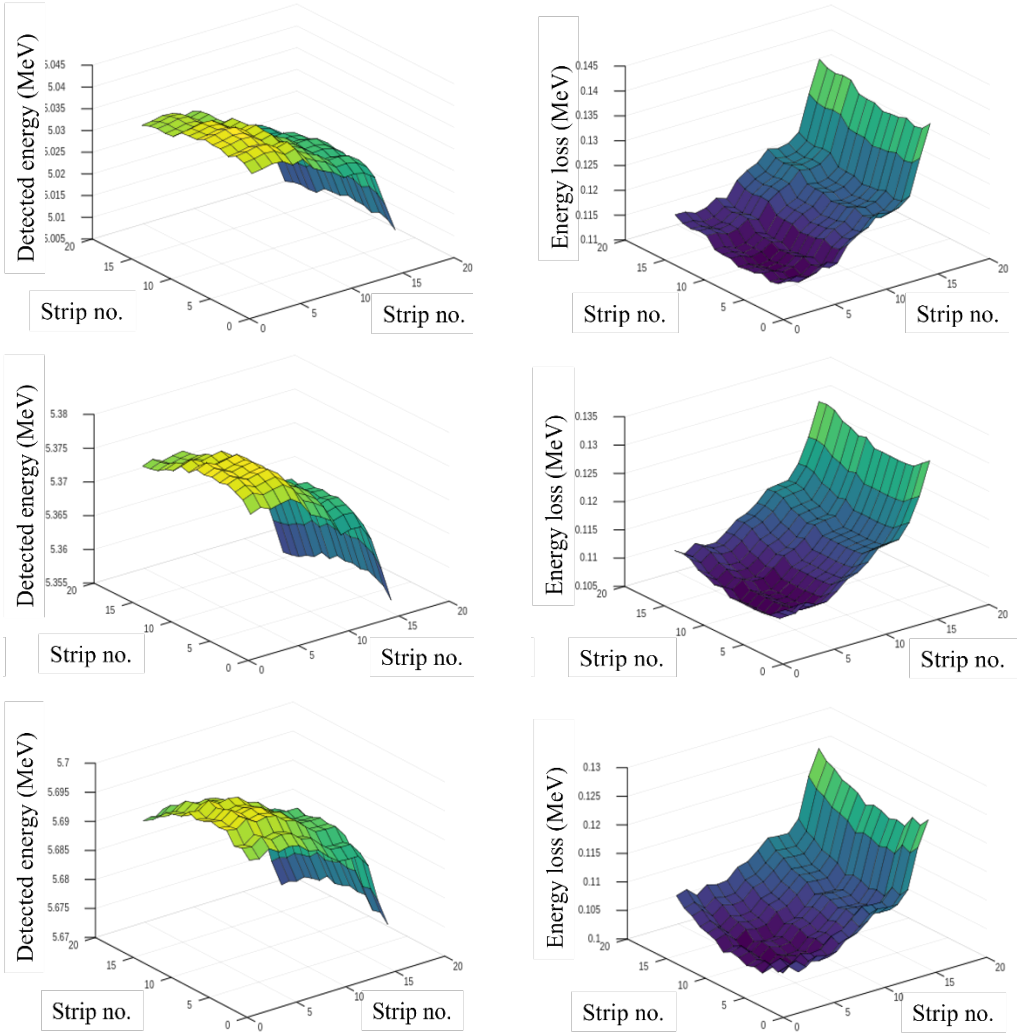

Fig. 5. The energy detected (left) and the energy loss (right) in the substrate for the first (up), the second (middle) and the third (down) peak of the alpha source.

Table 1

The energy loss for each peak and the corresponding thickness of the Mylar substrate

E_{loss} (keV)	Thickness (μm)	Thickness (μg/cm^2)
113.5 ± 3.3	0.968 ± 0.003	135.2 ± 3.9
109.7 ± 3.1	0.981 ± 0.003	137.0 ± 3.8
103.4 ± 1.6	0.9720 ± 0.0015	135.8 ± 2.0

The final thickness of the substrate is obtained as the mean of three values. Each value is determined from the pixel corresponding to the local extrema for the correspondent peak. The final uncertainty is the square root of the sum of the squares of those three uncertainties divided by three.

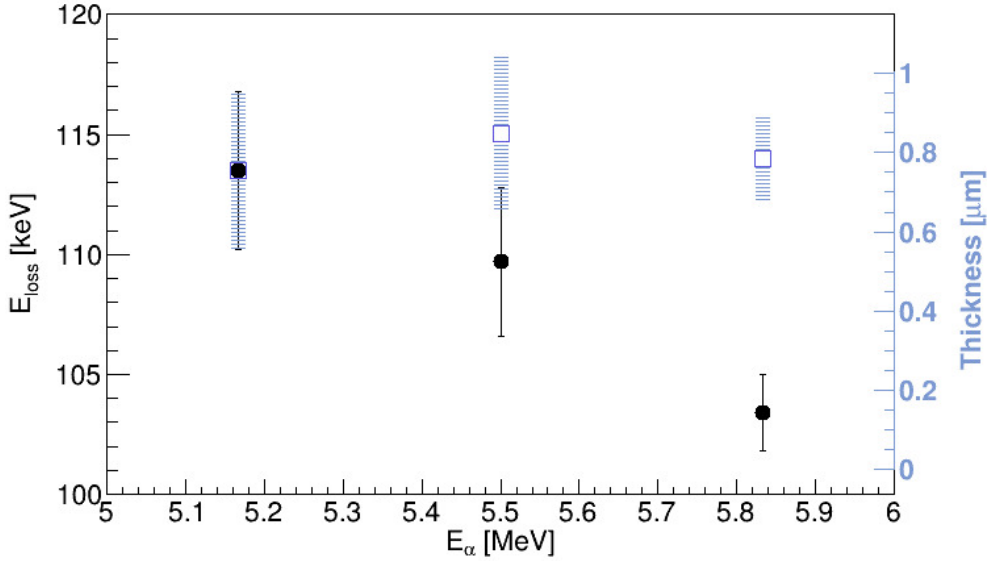

Fig. 6. The energy loss of alpha particles in the mylar substrate (black) and the associated thickness (blue). As the energy of the alpha particles is increasing, the energy loss in the substrate is decreasing. For all energy losses the associated thicknesses are in agreement.

The energy loss in the substrate is presented in Fig. 6 and Table 1 for each energy of the alpha source, together with the associated thicknesses. The final result of the measurement is 136.0 ± 1.9 μg/cm^2.

4.2 The measurement of the thickness of the LiF layers

The detected energy and the energy loss in each LiF layer were mapped for each energy of the alpha source. The targets were evaluated concomitantly to better emphasize the effect of the deviation. All the results corresponding to the second peak of the alpha source are presented together in Fig. 7. From the top (layer #1) to the bottom (layer #3), the effect of the deviation was decreasing. The layer #3 occupied the upper spot on the target holder and the local extrema are corresponding in this case to the central strips of the DSSSD. Near this upper spot the target holder was tightened on the linear manipulator, forcing it in a straight position. Therefore, the surface of the third target was almost parallel with the surface of the detector. However, the target holder was slightly curved and as getting closer to the lowest spot, the deviation angle between the plane of the target and the plane of the detector was increasing.

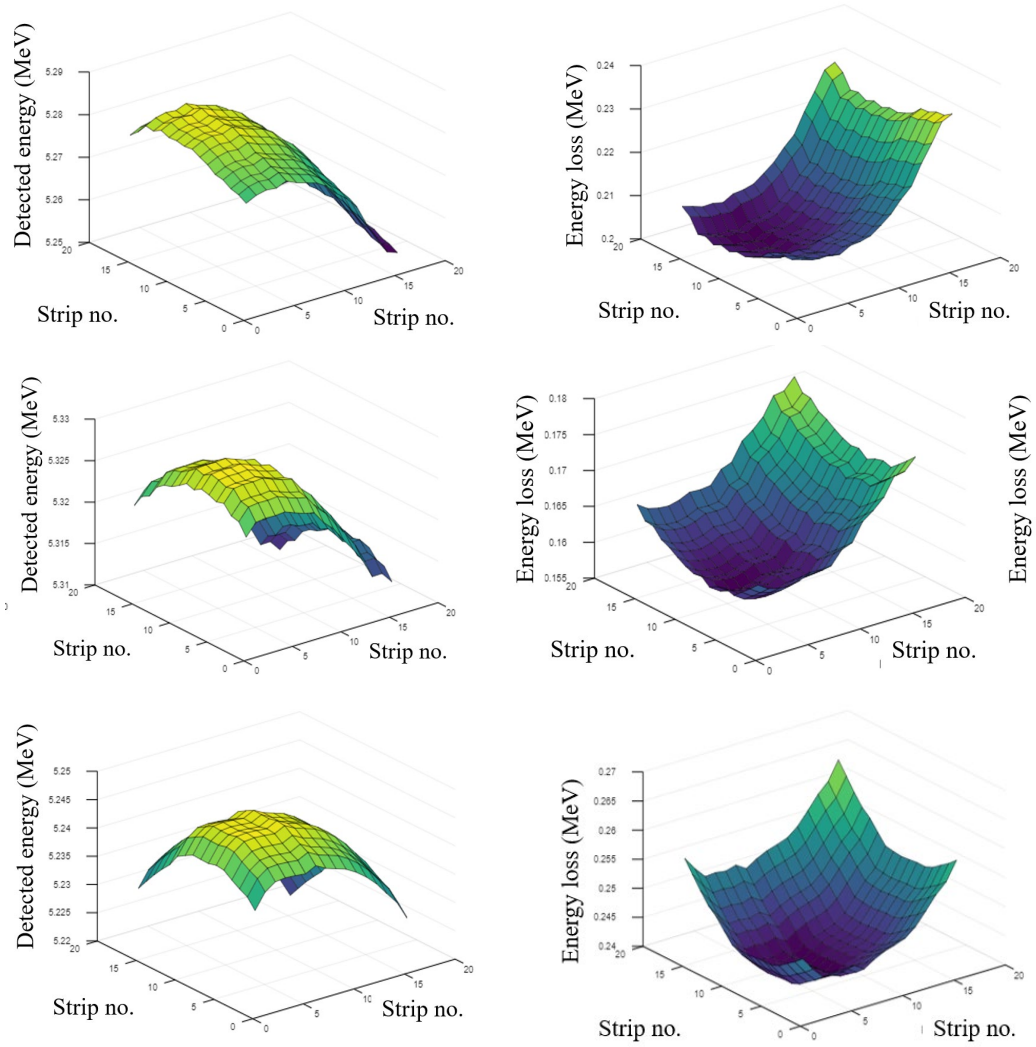

Fig. 7. The energy detected (left) after the 5.486 MeV alpha particles have passed through the layer #1 (up), layer #2 (middle) and layer #3 (down); The energy loss (right) of the 5.486 MeV alpha particles in the layer #1 (up), layer #2 (middle) and layer #3 (down)

For each layer, the thickness is determined by subtracting the value of the energy loss corresponding to the local extrema in the substrate from the value of the energy loss corresponding to the local extrema in the target. Therefore, the uncertainty of the thickness of the substrate is considered in the uncertainty of the thickness of the target.

The energy losses for each energy of the alpha source are presented in Fig. 8 for the substrate and for the three targets and the corresponding thicknesses are presented in Fig. 9. For layer #1, the minimum energy loss and the associated thicknesses are presented in Table 2. Equivalently, the correlation between the

minimum energy loss and the thickness is presented in Table 3 for the layer #2 and in Table 4 for the layer #3.

Table 2

The energy loss for each peak and the corresponding thickness of the LiF layer #1

E_{loss} - target (keV)	E_{loss} – layer (keV)	Thickness (μm)	Thickness (μg/cm^2)
212.1 ± 4.4	98.6 ± 7.3	0.53 ± 0.04	139.7 ± 10.3
204.4 ± 2.8	94.7 ± 5.6	0.53 ± 0.03	138.2 ± 8.2
194.7 ± 2.5	91.3 ± 4.0	0.53 ± 0.02	139.9 ± 6.1

Table 3

The energy loss for each peak and the corresponding thickness of the LiF layer #2

E_{loss} - target (keV)	E_{loss} – layer (keV)	Thickness (μm)	Thickness (μg/cm^2)
165.4 ± 3.0	51.9 ± 6.3	0.28 ± 0.03	73.0 ± 8.9
159.2 ± 2.4	49.5 ± 5.5	0.28 ± 0.03	72.5 ± 8.1
151.1 ± 1.4	47.7 ± 3.0	0.28 ± 0.02	73.4 ± 4.6

Table 4

The energy loss for each peak and the corresponding thickness of the LiF layer #3

E_{loss} - target (keV)	E_{loss} – layer (keV)	Thickness (μm)	Thickness (μg/cm^2)
251.0 ± 0.4	137.5 ± 3.7	0.74 ± 0.02	194.6 ± 5.2
241.4 ± 0.7	131.7 ± 3.8	0.73 ± 0.02	191.7 ± 5.5
230.2 ± 0.6	126.8 ± 2.2	0.735 ± 0.013	193.7 ± 3.4

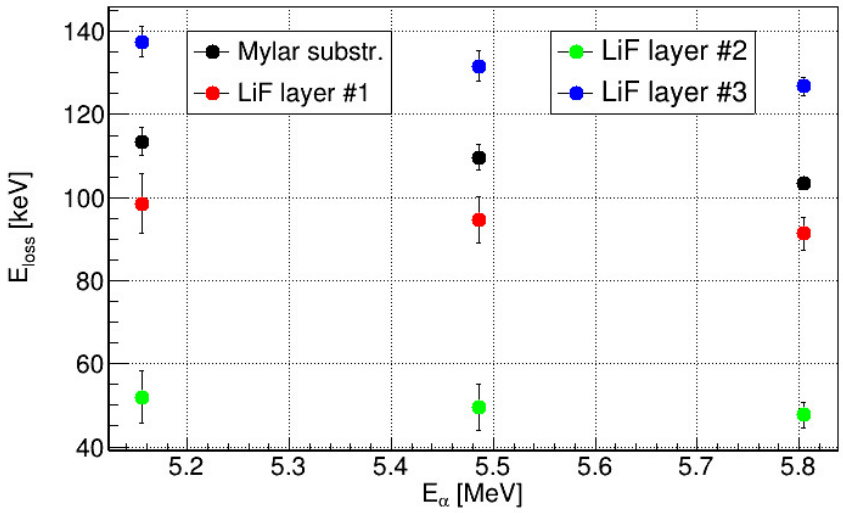

Fig. 8. The energy loss of the alpha particles through the Mylar substrate (black), LiF layer #1 (red), LiF layer #2 (green) and LiF layer #3 (blue) in function of the incident alpha energy

The thickness of the LiF layer #1 is 139.3 ± 4.7 μg/cm^2, the thickness of the LiF layer #2 is 73.0 ± 4.2 μg/cm^2 and the thickness of the LiF layer #3 is 193.3 ± 2.9 μg/cm^2. Therefore, while for the substrate the error of the measurement is around 1.44%, for the three layers the errors will be between 1.5% (for the thicker layer) and 5.8% (for the thinner layer).

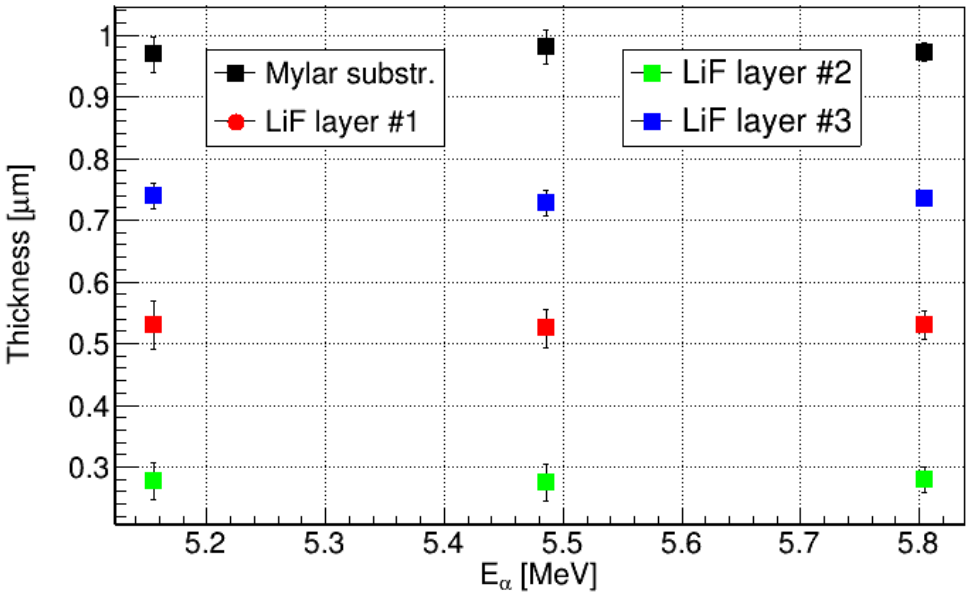

Fig. 9. The thickness corresponding to the energy loss of the alpha particles through the Mylar substrate (black), LiF layer #1 (red), LiF layer #2 (green) and LiF layer #3 (blue) in function of the incident alpha energy

A comparison between the results of the measurement and the values estimated by the Target Laboratory of LNS (INFN) through a similar measurement is presented in Table 5. In the INFN estimation the non-uniformity of the substrate was taken in account leading to a total uncertainty around 10% [20-21].

Table 5

The results of the measurements at ELI-NP compared with the values estimated by the INFN Target Laboratory (uncertainties around 10%)

	This work results (μg/cm^2)	INFN results (μg/cm^2)
Mylar substrate	136.0 ± 1.9	128
LiF layer #1	139.3 ± 4.7	131
LiF layer #2	73.0 ± 4.2	74
LiF layer #3	193.3 ± 2.9	201

5. Conclusions

A reliable procedure to determine the thickness and the uniformity of a target with a known stoichiometry by using a DSSSD, a standard alpha source and a basic data acquisition chain is proposed in this paper. The idea is grounded on the correlation between the lowest energy loss and the shortest path of the alpha particles through the target. The conversion of the energy units in length units is performed using LISE++ and SRIM/TRIM stopping power values. The implemented set-up has been used for routine measurements on several materials: Au, Ni, Mn, etc., but the results are not presented in this paper. The results of the measurement of the thickness of three LiF layers deposited on Mylar substrates have been reported. Moreover, a qualitative evaluation of the uniformity has been performed and it will be quantitatively explored in future measurements. The final results were successfully corrected to account for small misalignments in the experimental setup, thus revealing that the method can still be successfully applied. The thickness and the uniformity of the LiF layers will be used to estimate the number of ^{7}Li atoms available for the ^{7}Li(γ,α)^{3}H reaction at different energies and further the cross-section.

Acknowledgments

This work was supported by the Romanian Ministry of Research, Innovation and Digitalization under Contract PN 23.21.01.06 and the Institute of Atomic Physics Romania, Project ELIRO/DFG/2023−001 ARNPhot.

R E F E R E N C E S

[1] *C. Iliadis,* Nuclear Physics of Stars, Weinheim: Wiley-VCH, 2007.
[2] *V. Capirossi, F. Delaunay, F. Iazzi, F. Pinna, D. Calvo, M. Fisichella,* Thickness and uniformity characterization of thin targets for intense ion beam experiments, Acta Phys. Pol., Series B, Vol. 51, Iss. 3, 2020.
[3] *M. C. Fujiwara,* Thickness measurement of solid hydrogen thin film for muon catalyzed fusion via energy loss of alpha particles, Master Thesis, The University of British Columbia, 1994.
[4] *P.S. Morrall,* Target preparation method and characterization, Nucl. Instrum. Methods Phys. Res., Section A, Vol. 613, Iss. 3, 2010.
[5] https://tunl.duke.edu.

[6] *D. W. Bardayan, J. C. Blackmon, C. R. Brune, A. E. Champagne, A. A. Chen, J. M. Cox, T. Davinson, V. Y. Hansper, M. A. Hofstee, B. A. Johnson, R. L. Kozub, Z. Ma, P. D. Parker, D. E. Pierce, M. T. Rabban, A. C. Shotter, M. S. Smith, K. B. Swartz, D. W. Visser, P. J. Woods,* Observation of the Astrophysically Important 3^+ State in ^{18}Ne via Elastic Scattering of a Radioactive ^{17}F Beam from ^{1}H, Phys. Rev. Lett., Vol. 83, Iss. 1, 1999.

[7] https://www.lns.infn.it/en/targets.html.

[8] https://www.eli-np.ro/spectroscopy_lab.php.

[9] *J.E. Turner,* Atoms, Radiation and Radiation Protection – 3rd ed, Weinheim: Wiley-VCH, 2007.

[10] *G.F. Knoll,* Radiation Detection and Measurement – 3rd ed., John Wiley & Sons, 1999.

[11] *C. Yalçın*, Thickness measurement using alpha spectroscopy and SRIM, J. Phys. Conf. Ser., Vol. 590, 2015, DOI:10.1088/1742-6596/590/1/012050.

[12] *S. Agostinelli, J. Allison, K. Amako, J. Apostolakis, H. Araujo, P. Arce, M. Asai, D. Axen, S. Banerjee, G. Barrand, F. Behner, L. Bellagamba, J. Boudreau, L. Broglia, A. Brunengo, H. Burkhardt, S. Chauvie, J. Chuma, R. Chytracek, G. Cooperman, G. Cosmo, P. Degtyarenko, A. Dell'Acqua, G. Depaola, D. Dietrich, R. Enami, A. Feliciello, C. Ferguson, H. Fesefeldt, G. Folger, F. Foppiano, A. Forti, S. Garelli, S. Giani, R. Giannitrapani, D. Gibin, J.J. Gómez Cadenas, I. González, G. Gracia Abril, G. Greeniaus, W. Greiner, V. Grichine, A. Grossheim, S. Guatelli, P. Gumplinger, R. Hamatsu, K. Hashimoto, H. Hasui, A. Heikkinen, A. Howard, V. Ivanchenko, A. Johnson, F.W. Jones, J. Kallenbach, N. Kanaya, M. Kawabata, Y. Kawabata, M. Kawaguti, S. Kelner, P. Kent, A. Kimura, T. Kodama, R. Kokoulin, M. Kossov, H. Kurashige, E. Lamanna, T. Lampén, V. Lara, V. Lefebure, F. Lei, M. Liendl, W. Lockman, F. Longo, S. Magni, M. Maire, E. Medernach, K. Minamimoto, P. Mora de Freitas, Y. Morita, K. Murakami, M. Nagamatu, R. Nartallo, P. Nieminen, T. Nishimura, K. Ohtsubo, M. Okamura, S. O'Neale, Y. Oohata, K. Paech, J. Perl, A. Pfeiffer, M.G. Pia, F. Ranjard, A. Rybin, S. Sadilov, E. Di Salvo, G. Santin, T. Sasaki, N. Savvas, Y. Sawada, S. Scherer, S. Sei, V. Sirotenko, D. Smith, N. Starkov, H. Stoecker, J. Sulkimo, M. Takahata, S. Tanaka, E. Tcherniaev, E. Safai Tehrani, M. Tropeano, P. Truscott, H. Uno, L. Urban, P. Urban, M. Verderi, A. Walkden, W. Wander, H. Weber, J.P. Wellisch, T. Wenaus, D.C. Williams, D. Wright, T. Yamada, H. Yoshida, D. Zschiesche,* Geat4 - a simulation toolkit, Nucl. Instrum. Methods Phys. Res., Section A, Vol. 506, Iss. 3, 2003.

[13] *J. F. Ziegler, M.D. Ziegler, J.P. Biersack,* SRIM – The stopping and range of ions in matter, Nucl. Instrum. Methods Phys. Res., Section B, Vol. 268, Iss. 11-12, 2010.

[14] *O.B. Tarasov, D. Bazin,* LISE++: Radioactive beam production with in-flight separators, Nucl. Instrum. Methods Phys. Res., Section B, Vol. 266, Iss. 19-20, 2008.

[15] *J. Baró, J. Sempau, J.M. Fernández-Varea, F. Salvat,* PENELOPE: An algorithm for Monte Carlo simulation of the penetration and energy loss of electrons and positrons in matter, Nucl. Instrum. Methods Phys. Res., Section B, Vol. 100, Iss. 1, 1995.

[16] https://www.micronsemiconductor.co.uk.

[17] https://www.mesytec.com.

[18] https://www.ortec-online.com.

[19] *J.W. Eaton, D. Bateman, S. Hauberg,* GNU Octave: A high-level interactive language for numerical computations, Network Theory Limited, 2008.

[20] *M. Fisichella, A. Massara., M. Giovannini,* Production and characterization of molybdenum /HOPG thin targets for the NUMEN experiment, Eur. Phys. J., Series A, Vol. 61, No. 144, 2025.

[21] *A. Massara, M. Fisichella, M. Ursino, V. Capirossi, F. Cappuzzello, M. Cavallaro, F. Delaunay, F. Pinna, A. Rovelli for the NUMEN collaboration*, Preparation and characterization of High Oriented Pyrolytic Graphite backed targets for the NUMEN project, EPJ Web Conf., Vol. 285, 2023.